Upwind Navier-Stokes Solutions for Separated Periodic Flows

Christopher L. Rumsey,* James L. Thomas,* Gary P. Warren,* and Grace C. Liu*
NASA Langley Research Center, Hampton, Virginia

The application of an upwind implicit approximate factorization Navier-Stokes algorithm to highly separated flow is described. Using both the thin-layer and complete forms of the Navier-Stokes equations, the low Reynolds number laminar flow around a circular cylinder with periodic shedding is solved. The effects of grid density, grid extent, and time step on the Strouhal number are shown. Results from both sets of equations agree within the experimental data band. Unsteady, laminar flow computations for inclined plates and airfoils are also described. Strouhal numbers agree to within 5% of experiments for inclined plates. Differences between solutions of the complete equations and the thin-layer approximation for separated periodic flows are discussed. Computations of an impulsively started circular cylinder yield time-accurate flowfields in good agreement with experimental flow visualizations. The turbulent Reynolds-averaged computation of an airfoil at a high angle of attack of 25 deg is massively separated, but it shows little evidence of periodicity.

Nomenclature

a = speed of sound; also distance of bubble center behind cylinder
A, B, M, N = Jacobian matrices
b = height of bubble center above centerline of cylinder
c = airfoil chord (taken to be unity)
c_d = section drag coefficient
c_f = coefficient of friction
c_ℓ = section lift coefficient
c_p = pressure coefficient
d = cylinder diameter (taken to be unity)
e = total energy, nondimensionalized by $\rho_\infty a_\infty^2$
G, H = fluxes of mass, momentum, and energy
h = $1/(\sqrt{NJ^* NK})$
I = identity matrix
J = transformation Jacobian; also index for direction along body
K = index for direction outward from body; also stretching factor
ℓ = characteristic length: d for cylinder, c for airfoil or plate; also length of separation bubble
M = freestream Mach number
n = shedding frequency
NJ = number of grid points along body, in J direction
NK = number of grid points outward from body, in K direction
p = pressure, nondimensionalized by $\rho_\infty a_\infty^2$
Pr = Prandtl number
Q = conservation variables
r = distance outward from body
R, S = viscous terms of the Navier-Stokes formulation
Re = Reynolds number, $\rho_\infty u_\infty \ell/\mu_\infty$
$\overline{Re}$ = Reynolds number, $\rho_\infty a_\infty \ell/\mu_\infty$
RHS = right-hand side term of Navier-Stokes equation
St = Strouhal number, $n\ell \sin\alpha/u_\infty$
t = time, nondimensionalized by ℓ/a_∞
u, v = Cartesian velocities in x and y directions, respectively, nondimensionalized by a_∞
x, y = Cartesian coordinates
α = angle of attack
β = stretching function parameter
γ = ratio of specific heats
ΔQ = $Q^{n+1} - Q^n$
Δt = time step
η, ζ = general curvilinear coordinates
λ = coefficient of bulk viscosity
μ = coefficient of molecular viscosity
ρ = density, nondimensionalized by ρ_∞
$\tau_{xx}, \tau_{xy}, \tau_{yy}$ = viscous shear stress terms

Subscripts

max = maximum
min = minimum
x, y = differentiation in x and y directions, respectively
η, ζ = differentiation in η and ζ directions, respectively
∞ = conditions at infinity

Superscripts

n = time level
$\hat{}$ = quantities in generalized coordinates
$\pm$ = positive and negative flux contributions

Presented as Paper 86-0247 at the AIAA 24th Aerospace Sciences Meeting, Reno, NV, Jan. 6-9, 1986; received Feb. 19, 1986; revision received Aug. 25, 1986.

*Research Scientist, Low-Speed Aerodynamics Division. Member AIAA.

Introduction

THE study of unsteady viscous flow problems is a fundamental aspect of classical aerodynamics that does not easily lend itself to computational analysis because of inherent turbulence, massive flow separation, and strong viscous/inviscid interaction. However, it is important to attempt to solve these types of flows since a large number of problems of practical importance are unsteady. For example, flows around

bluff bodies such as cables, external stores, or buildings are generally unsteady and periodic in nature. At high angles of attack past stall, airfoils exhibit similar characteristics. The successful analysis of high-angle-of-attack airfoil flows would enable prediction of maximum lift coefficient and stall angle for use in performance studies, as well as determine the unsteady lift, moment, and flowfield for use in dynamic stability and control studies.

Extensive experimental results for unsteady flow around circular cylinders and high-angle-of-attack flat plates are available in the literature. These include the experiments and documentation of Thom,[1] Morkovin,[2] and Roshko[3] for cylinders and of Fage and Johansen[4] and Tyler[5] for flat plates. Cylinders shed alternating vortices with a constant Strouhal number of approximately 0.21 between Reynolds numbers of about 200 to 10^5; Strouhal numbers are lower below this range and higher past Reynolds numbers of 10^5. Fage and Johansen measured Strouhal numbers of approximately 0.15 at all angles of attack between 28 and 90 deg for flat plates at Reynolds numbers between about $3*10^4$ and $1.5*10^5$. Tyler's experiments yielded a Strouhal number of about 0.158 at all angles of attack between 20 and 90 deg, for Reynolds numbers between about 200 and 7000.

Jones[6] found qualitatively that some airfoils exhibit a large range of lift coefficients at a constant angle of attack just past the stall angle but show fewer oscillations at slightly higher angles. Tyler[5] determined a general Strouhal number of about 0.150 for airfoils between 20- and 90-deg angles of attack, at Reynolds numbers between about 200 and 7000.

Computational studies have been performed on separated airfoil flows. Ghia, Osswald, and Ghia[7,8] used the incompressible form of the Navier-Stokes equations in terms of vorticity and stream function to analyze the unsteady laminar flow over a 12%-thick Joukowski airfoil at 5, 15, and 30 deg. Lecointe and Piquet[9] used several compact schemes with the Navier-Stokes vorticity/stream-function formulation to solve for the laminar flows around circular cylinders and airfoils.

Rumsey[10] used a central-difference, thin-layer Navier-Stokes code developed by Pulliam et al.[11] to predict the flow around low Reynolds number circular cylinders and high Reynolds number turbulent airfoils past stall. The airfoil results agreed qualitatively with Jones' description of stalled flow. In addition, an implicit upwind Navier-Stokes code using conserved flow variables and flux-vector splitting was introduced and used to analyze laminar circular cylinder flow.

The present paper continues the investigation of separated periodic flows using the implicit upwind Navier-Stokes code presented in Ref. 10. A thorough investigation of low Reynolds number circular cylinder flow is conducted using both thin-layer and complete Navier-Stokes formulations, including effects of spatial and temporal grid refinement and grid extent. Separated laminar inclined plate solutions are compared with experiment, and several unsteady laminar flows over airfoils are presented. Finally, a turbulent solution for a stalled airfoil is included.

Governing Equations

The two-dimensional Reynolds-averaged Navier-Stokes equations can be written using generalized coordinates as

$$\frac{\partial \hat{Q}}{\partial t}+\frac{\partial \hat{G}}{\partial \eta}+\frac{\partial \hat{H}}{\partial \zeta}=\overline{Re}^{-1}\left\{\partial_\eta\left[J^{-1}\left(\eta_x R+\eta_y S\right)\right]+\partial_\zeta\left[J^{-1}\left(\zeta_x R+\zeta_y S\right)\right]\right\} \tag{1}$$

$$\hat{Q}=Q/J \tag{2a}$$

$$\hat{G}=\left(\eta_x G+\eta_y H\right)/J \tag{2b}$$

$$\hat{H}=\left(\zeta_x G+\zeta_y H\right)/J \tag{2c}$$

$$Q=\begin{bmatrix}\rho\\ \rho u\\ \rho v\\ e\end{bmatrix}\qquad G=\begin{bmatrix}\rho u\\ \rho u^2+p\\ \rho uv\\ u(e+p)\end{bmatrix}\qquad H=\begin{bmatrix}\rho v\\ \rho uv\\ \rho v^2+p\\ v(e+p)\end{bmatrix} \tag{3}$$

$$p=(\gamma-1)\left[e-0.5\rho\left(u^2+v^2\right)\right] \tag{4}$$

where η is the coordinate along the body and ζ is the coordinate normal to the body.

The viscous terms on the right-hand side are given by

$$R=\begin{bmatrix}0\\ \tau_{xx}\\ \tau_{xy}\\ R_4\end{bmatrix}\qquad S=\begin{bmatrix}0\\ \tau_{xy}\\ \tau_{yy}\\ S_4\end{bmatrix} \tag{5}$$

$$\tau_{xx}=(\lambda+2\mu)\left(\eta_x u_\eta+\zeta_x u_\zeta\right)+\lambda\left(\eta_y v_\eta+\zeta_y v_\zeta\right) \tag{6a}$$

$$\tau_{yy}=(\lambda+2\mu)\left(\eta_y v_\eta+\zeta_y v_\zeta\right)+\lambda\left(\eta_x u_\eta+\zeta_x u_\zeta\right) \tag{6b}$$

$$\tau_{xy}=\mu\left(\eta_y u_\eta+\zeta_y u_\zeta+\eta_x v_\eta+\zeta_x v_\zeta\right) \tag{6c}$$

$$R_4=u\tau_{xx}+v\tau_{xy}+\mu Pr^{-1}(\gamma-1)^{-1}\left(\eta_x\partial_\eta a^2+\zeta_x\partial_\zeta a^2\right) \tag{6d}$$

$$S_4=u\tau_{xy}+v\tau_{yy}+\mu Pr^{-1}(\gamma-1)^{-1}\left(\eta_y\partial_\eta a^2+\zeta_y\partial_\zeta a^2\right) \tag{6e}$$

Stokes hypothesis, $\lambda=-\frac{2}{3}\mu$, is used for bulk viscosity. The coordinate transformation Jacobian is given by

$$J=\eta_x\zeta_y-\eta_y\zeta_x \tag{7}$$

$$\eta_x=Jy_\zeta,\quad \eta_y=-Jx_\zeta,\quad \zeta_x=-Jy_\eta,\quad \zeta_y=Jx_\eta \tag{8}$$

The thin-layer assumption can be made when the viscous terms associated with derivatives tangent to the body are considered negligible. The thin-layer equations are the same as Eqs. (1-6), except that all derivatives with respect to η on the right-hand side are zero (including all η derivatives in R and S).

An implicit, upwind, finite-volume scheme described by Rumsey[10] is used to solve Eq. (1). Application of approximate factorization allows the system of equations to be solved in two sweeps:

$$\left[\frac{I}{J\Delta t}+\partial_\eta^- A^+ +\partial_\eta^+ A^- -\overline{Re}^{-1}\partial_\eta J^{-1}N\right]\Delta Q^*=-\mathrm{RHS} \tag{9a}$$

$$\left[\frac{I}{J\Delta t}+\partial_\zeta^- B^+ +\partial_\zeta^+ B^- -\overline{Re}^{-1}\partial_\zeta J^{-1}M\right]\Delta Q=\frac{\Delta Q^*}{J\Delta t} \tag{9b}$$

$$\mathrm{RHS}=\partial_\eta^-\hat{G}^+ +\partial_\eta^+\hat{G}^- +\partial_\zeta^-\hat{H}^+ +\partial_\zeta^+\hat{H}^- -\overline{Re}^{-1}\times\left\{\partial_\eta\left[J^{-1}\left(\eta_x R+\eta_y S\right)\right]+\partial_\zeta\left[J^{-1}\left(\zeta_x R+\zeta_y S\right)\right]\right\} \tag{10}$$

The + and − superscripts indicate flux split quantities, according to the flux vector splittings of Van Leer.[12] A and B are linearizations of the G and H fluxes, and M and N arise from the linearizations of viscous terms in the ζ direction and η direction, respectively. All viscous terms are centrally dif-

ferenced, and implicit cross-derivative terms are neglected in the formulation. This algorithm is accurate to first order in time, and second order in space. Implicit spatial derivatives of the convective and pressure terms are first-order accurate.

Considerable computational time can be saved by updating the A, B, M, and N matrices once every set number of iterations, generally specified as twenty in the present study. This procedure has been found to yield identical results to continuous updating for unsteady solutions, provided that the period of unsteady oscillation is considerably greater than the number of iterations to update.

The thin-layer Navier-Stokes equations are similar to Eqs. (9a) and (9b), again with the exception that there are no η derivatives in the viscous terms in RHS and there is no implicit viscous term addition in the first sweep. Since this is an upwind scheme, no artificial dissipation is necessary, and there are no dissipation parameters to adjust. For turbulent calculations, the two-layer algebraic eddy viscosity model of Baldwin and Lomax[13] is employed as a turbulence model.

Boundary conditions are applied explicitly. No-slip, adiabatic wall conditions, as well as zero pressure conditions, are applied to the body:

$$u = v = 0 \tag{11a}$$

$$\frac{\partial p}{\partial \zeta} = \frac{\partial a^2}{\partial \zeta} = 0 \tag{11b}$$

where a^2 is proportional to the temperature. In the far field, the subsonic freestream boundary conditions are determined through a characteristic analysis normal to the boundary, and a point vortex representation for induced velocities on the outer boundary is included. Details can be found in Thomas and Salas.[14]

For some cases, flux limiting is employed in order to limit the differences used in the state variable interpolations to cell interfaces, enabling larger time steps to be taken in regions of high gradients. A description of the continuously differentiable limiter used can be found in Anderson et al.[15]

Results

In the initial part of the present study, steady-state computations were performed for code validation. One of these is detailed in the present paper in order to establish the accuracy of the code. A summary of the unsteady, time-accurate computations is given in Table 1. Four general categories of unsteady flow are analyzed: laminar circular cylinder flow, laminar inclined flat-plate flow, laminar airfoil flow, and turbulent airfoil flow.

The present code is fully vectorized for the VPS-32 computer. The computational speed of the code is approximately 14.5 μs/grid point/time step for laminar thin-layer Navier-Stokes solutions, 15.5 μs/grid point/time step for turbulent thin-layer Navier-Stokes solutions, and 16.5 μs/grid point/time step for laminar complete Navier-Stokes solutions.

Steady-State Results

The RAE 2822 airfoil was analyzed on a 265 × 101 C-mesh with an outer boundary extent of 20 chords. The algebraic turbulence model of Baldwin and Lomax[13] is employed beyond the location of experimental transition strips ($x/c = 0.03$) on the airfoil; in front of this point, laminar flow is assumed. The pressure and skin-friction distributions are compared in Fig. 1 to experimentally determined values (Cook et al.[16]), as well as to results from the thin-layer central-difference Navier-Stokes code of Swanson et al.[17] Both methods show good agreement with experiment over the entire airfoil and predict the location of the upper surface shock in close agreement with the experimental location. The value of lift obtained with the present method is 0.816, while the method of Swanson gives 0.820. The experimental value is 0.803. The effect of the far-field boundary extent on the computed lift coefficient has been investigated. The lift coefficient increases by 3% from 0.7845 to 0.8101 when the outer boundary is moved from 10 to 15 chords. With an outer boundary extent of $20c$, the lift coefficient is 0.8157, an increase of only 0.7% from the result using the $15c$ extent grid. Note that the experimental results were obtained at $\alpha = 3.19$ deg; the angle of attack of 2.79 deg used in the computations is the wall-corrected angle based on linear theory.

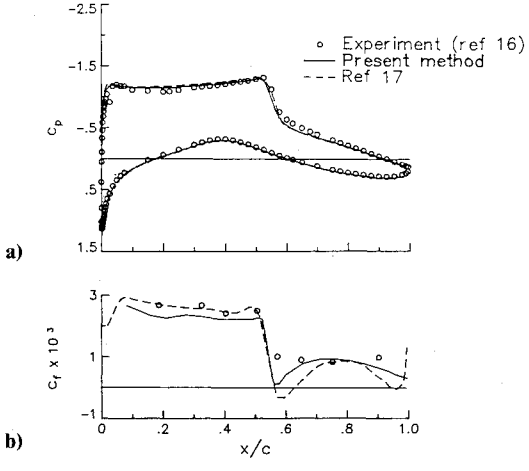

Fig. 1 RAE 2822 airfoil: $\alpha = 2.79$ deg; $M = 0.73$; $Re = 6.5 * 10^6$. a) pressure distribution; b) upper surface friction coefficient.

Table 1 Unsteady Navier-Stokes computations

α deg	M	Re	N-S Eq.	Grid	Δr_{min}	r_{max}	Δt	c_ℓ range	St	Experiment
Circular cylinder										
0	0.3	174	Thin-layer	—	—	—	—	−0.8-0.8	0.195	Ref. 2, $St = 0.174$
0	0.3	174	Complete	—	—	—	—	−0.6-0.6	0.189	to 0.196
0	0.3	200	Thin-layer	101 × 101	0.00056	20	0.05	—	—	Ref. 19, startup
Flat plate										
20	0.3	1000	Thin-layer	193 × 65	0.001	20	0.005	0.83-0.94	0.152	Ref. 4, $St = 0.164$-0.172
30	0.3	1000	Thin-layer	193 × 65	0.001	20	0.005	0.95-1.4	0.150	Ref. 4, $St = 0.153$
12% Joukowski airfoil										
15	0.4	1000	Thin-layer	214 × 43	0.00125	8	0.05	0.51-0.85	0.136	—
15	0.4	1000	Complete	214 × 43	0.00125	8	0.05	0.50-0.82	0.133	—
30	0.3	1000	Thin-layer	161 × 45	0.00086	10	0.01	.92/.96-1.17/1.22	0.166	—
53	0.3	1000	Thin-layer	161 × 45	0.00086	10	0.01	0.95-1.27	0.166	—
NACA 0012 airfoil										
20	0.3	3000	Thin-layer	151 × 40	0.0001	10	0.01	0.69-0.74	0.163	—
20	0.3	20,000	Thin-layer	151 × 40	0.0001	10	0.002	0.63-0.67	0.175	—
20	0.3	350,000	Thin-layer	151 × 40	0.0001	10	0.002	0.60-0.67	0.168	—
25	0.3	1 million	Thin-layer	201 × 65	0.00004	10	0.001	$c_\ell = 1.07$	—	Ref. 21, $c_\ell = 1.0$

Unsteady Laminar Circular Cylinder Flow

An extensive grid refinement study was conducted for unsteady laminar circular cylinder flow at a Reynolds number of 174, and thus only two results are listed in Table 1—one for thin-layer and one for complete Navier-Stokes equations. The results correspond to Strouhal numbers for an infinitely fine mesh extending to infinity, using an infinitely small time step. Note that 25 computations were made in order to obtain these results. Three grid sizes, 151×76, 166×84, and 201×101, were used with systematic variations in outer boundary extent and time step as described below.

An O-mesh topology for the cylinder flow is used with uniform spacing of the radial ($J = \text{const}$) lines, and with exponential stretching of the circumferential ($K = \text{const}$) lines. In order to ensure that the grid spacing approaches zero uniformly throughout the mesh as it is refined, the variable grid scheme of Blottner[18] is used:

$$r_J = r_{NJ} * (K^{\beta(J-1)} - 1)/(K^{\beta(NJ-1)} - 1) \qquad (12)$$

where

$$\beta = (NJ_{\text{ref}} - 1)/(NJ - 1) \qquad (13)$$

NJ_{ref} is the number of grid points in the J direction of the reference grid (which is subsequently to be refined), and K is the geometric stretching factor, typically on the order of 1.1. An earlier study performed by Rumsey[10] for this same case resolved the grid spacing only normal to the body. The present results are an extension of this study, since grid spacing is refined in both the normal and tangential directions.

Figure 2 shows example lift-coefficient time histories for the thin-layer and complete Navier-Stokes solutions, using a time step of 0.1 on identical grids (166×84) at a Reynolds number of 174. The solutions are periodic: the thin-layer equations predict a Strouhal number of 0.170, while the complete equations predict 0.164 for this case. The magnitude of the maximum-to-minimum lift range is higher for thin-layer than complete equations by about 30%. Note that on this and all subsequent time-history plots, the nondimensional times given on the abscissa are for reference only and do not necessarily reflect the amount of time taken to reach the point shown. All unsteady computations are made until a repeatable limit cycle is reached—only these repeatable cycles are shown. In the case of the circular cylinder for meshes with uniform spacing of the radial lines, it is necessary to perturb the solution (by introducing a v-velocity component at one instant in time early in the evolution of the flow) in order to obtain a periodic, as opposed to steady, solution.

The effect of grid refinement on Strouhal number for the thin-layer equations is shown in Fig. 3 for three grid extents and a fixed time step of 0.1. The linear relationship between Strouhal number and h^2 confirms the second-order spatial accuracy of the solution. Increasing the grid extent decreases the Strouhal number, and increasing the grid density increases the Strouhal number. The stretching factor for the coarsest grid, K_{ref}, is chosen to ensure that approximately 20 points lie in the laminar boundary layer. The 20-diameter solution was run with grids using two different stretching factors. The lower stretching factor gives a higher Strouhal number for a given number of grid points, but both extrapolate to the same Strouhal number for an infinitely refined mesh. Notice that the coarsest mesh (151×76) with a grid extent of $20d$ gives a Strouhal number approximately 9% in error from that of an infinitely refined grid with the same grid extent. Figure 4 depicts a similar grid refinement study at a time step of 0.1 for the complete Navier-Stokes solution. Again, the results confirm that the algorithm is second-order accurate in space, and the trends are very similar to those described above for the thin-layer solutions.

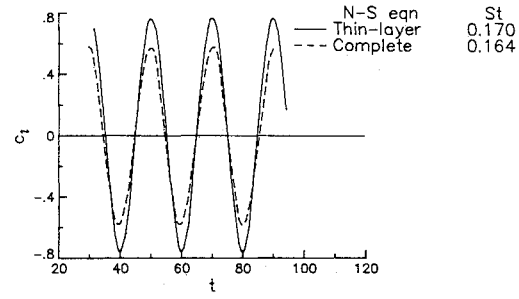

Fig. 2 Circular cylinder lift-coefficient time history; $M = 0.3$; $Re = 174$.

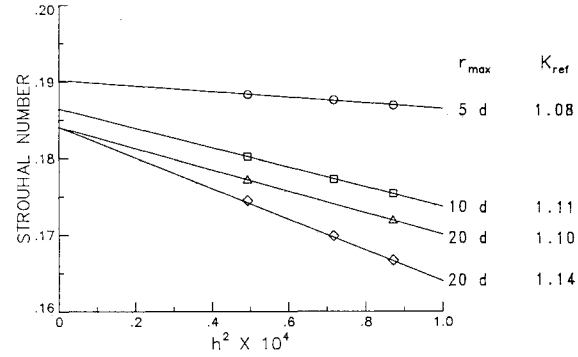

Fig. 3 Effect of grid refinement on Strouhal number for circular cylinder using thin-layer N-S; $M = 0.3$; $Re = 174$.

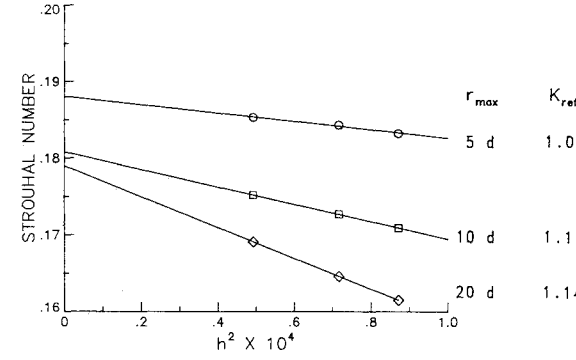

Fig. 4 Effect of grid refinement on Strouhal number for circular cylinder using complete N-S; $M = 0.3$; $Re = 174$.

The effect of outer boundary extent and time step is shown in Fig. 5. The results at a time step of 0.1 corresponding to $h^2 \to 0$ from Figs. 3 and 4 are shown. In addition, the circular cylinder was analyzed on the 201×101 grid at a lower time step of 0.05 for both the $10d$ and $20d$ grid extents, in order to determine the effect of time step on the Strouhal number. The lower time step was found to increase Strouhal number in both cases. Since the present method is known to be first-order accurate in time, the Strouhal number corresponding to an infinitesimally small time step and infinitely refined mesh can be extrapolated by assuming that the same spatial dependence of Strouhal number shown in Figs. 3 and 4 applies to the solutions refined in time. Results at an extrapolated time step of zero shown in Fig. 5 are about 7% higher than results for a time step of 0.1. The thin-layer Navier-Stokes solutions produce Strouhal numbers slightly higher (3%) than those given by the complete equations, although both fall within the band of experimental results (from Morkovin[2]).

Computations using the thin-layer Navier-Stokes equations are compared with experiment for a cylinder at a Reynolds number of 200 at small times after an impulsive start. A

101 × 101 half-cylinder mesh is used, with symmetry enforced along the centerline. The time step is 0.05. Figure 6a shows the wake bubble parameters ℓ/d, a/d, and b/d in comparison to the experiment of Bouard and Coutanceau.[19] Theory shows good agreement with experiment. Figure 6b shows stream-function contours of the solution at time $t = 8.35$.

Unsteady Laminar Inclined Flat-Plate Flow

Fage and Johansen[4] determined experimental Strouhal numbers for a flat plate at high angles of attack. The plate, tested at Reynolds numbers of about 150,000, had sharp edges and was flat on one face, with a small amount of thickness (3% at midchord) on the other. In the present study, an O-mesh is used to model this shape, and two angles of attack at a Reynolds number of 1000 are analyzed. In both experiment and computation, the flat side of the plate faces toward the oncoming flow. The Reynolds number of the computation is lower than that of the experiment; however, Fage and Johansen found the Strouhal number to be relatively insensitive to Reynolds number. A Reynolds number sensitivity study for an airfoil, described in the next section, supports this hypothesis as well.

Table 1 summarizes the computed results for the inclined plate at angles of attack of 20 and 30 deg, and Fig. 7 shows the corresponding lift-coefficient time histories. Both thin-layer solutions have very regular periodic natures. Strouhal numbers for the 20- and 30-deg cases are 0.152 and 0.150, respectively. The 30-deg result agrees very well with the experimental value of 0.153 determined by Fage and Johansen, but the 20-deg result is slightly lower than the measured values of 0.164-0.172. Tyler[5] determined a general Strouhal number of 0.158 for flat plates from 20- to 90-deg angle of attack, in close agreement with the present results.

Pressure coefficients, averaged over approximately two cycles, are compared with experimental values in Fig. 8 for the 30-deg case. Agreement is excellent everywhere except on the upper surface near the leading and trailing edges, where theory predicts small pressure peaks not present in the experimental data. It should be noted that experimental data for the upper surface was obtained by inverting the plate and allowing the flat surface (which contained the pressure taps) to face away from the oncoming flow.

Unsteady Laminar Airfoil Flow

Calculations using the thin-layer equations are made for the NACA 0012 airfoil at an angle of attack of 20 deg for three different Reynolds numbers: 3000, $2*10^4$, and $3.5*10^5$. The same 151 × 40 grid is used for each case. Its minimum normal spacing is small enough to allow for 10-20 grid points in the laminar boundary layer at the highest Reynolds number. The lift variation with time is shown in Fig. 9. The highest lift values are obtained at the lowest Reynolds number, and the magnitudes of the minimum-to-maximum lift-coefficient variation in the limit cycles are different for each Reynolds number. However, the Strouhal number changes very little, giving 0.163, 0.175, and 0.168 for the lowest to the highest Reynolds number. This represents a maximum change in Strouhal number of about 7% over this wide range of laminar flow Reynolds numbers. These Strouhal numbers are comparable to the general Strouhal number of about 0.150 given by Tyler[5] for airfoils between 20- and 90-deg angle of attack.

The 12% Joukowski airfoil was analyzed using the thin-layer equations for a Reynolds number of 1000 at three different angles of attack. A 214 × 43 grid (with 100 points on the airfoil surface) is used for the unsteady 15-deg solution. This allows for direct comparison with the results of Ghia et al.[7] The other two angles of attack are analyzed on a 161 × 45 grid, with 87 points on the airfoil surface. Lift-coefficient time histories are shown in Fig. 10. The 15-deg case yields lower values of lift than both the higher angles. Strouhal numbers are 0.136, 0.166, and 0.166 for the 15-, 30-, and 53-deg configurations, respectively.

For the 15-deg case, the Strouhal number obtained using the thin-layer Navier-Stokes equations is 2% higher than that using the complete equations on the same grid, and the minimum-to-maximum lift range is higher, as seen in Fig. 11. These trends are similar to the earlier results for the circular cylinder. It appears that even at low Reynolds numbers (as evidenced by results at $Re = 174$ for cylinders and $Re = 1000$ for airfoils) the thin-layer equations can predict Strouhal numbers for unsteady flows to within a few percent of the complete equations, but the lift values can be in error by as much as 30% at the maximum and minimum lift locations.

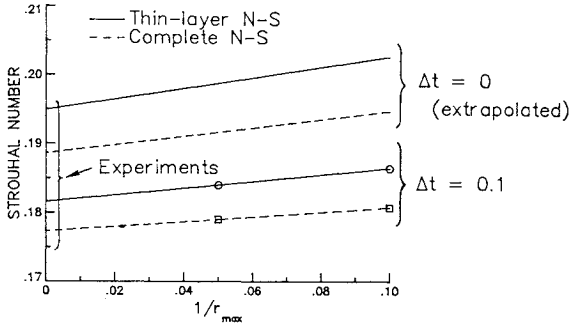

Fig. 5 Effect of outer boundary and time step on Strouhal number for circular cylinder; $M = 0.3$; $Re = 174$.

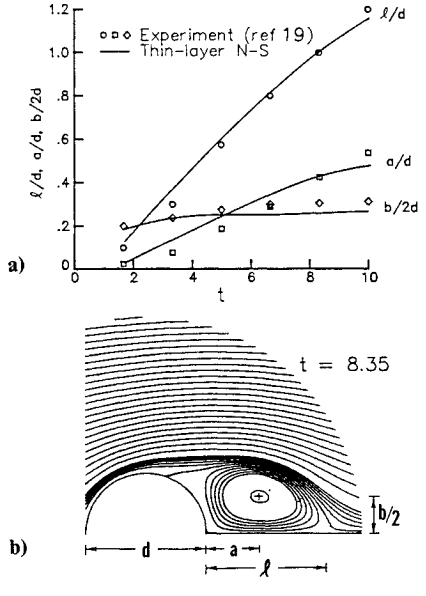

Fig. 6 Startup computation for circular cylinder; $M = 0.3$; $Re = 200$. a) wake bubble parameters; b) stream-function contours.

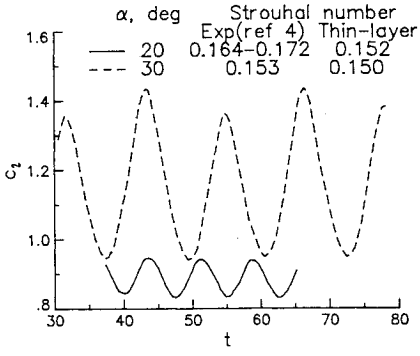

Fig. 7 Lift-coefficient time history for inclined plate; $M = 0.3$; $Re = 1000$.

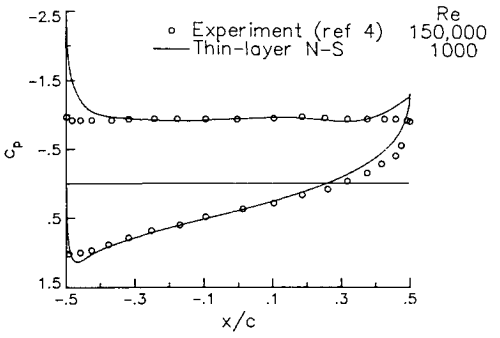

Fig. 8 Mean pressure distribution for inclined plate; $\alpha = 30$ deg; $M = 0.3$.

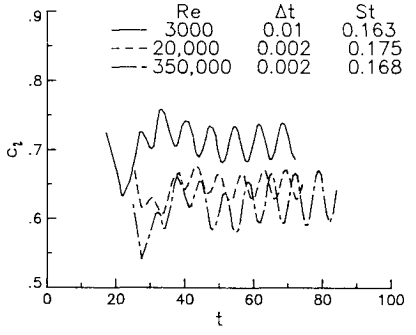

Fig. 9 Lift-coefficient time history for NACA 0012 airfoil; $\alpha = 20$ deg; $M = 0.3$.

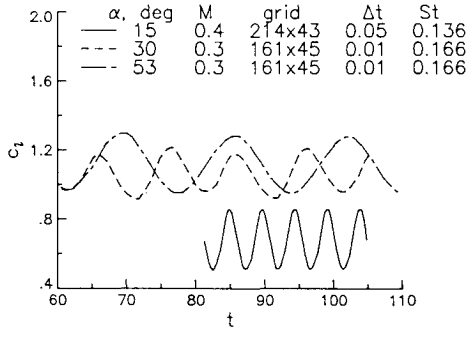

Fig. 10 Lift-coefficient time history for 12% Joukowski airfoil; $Re = 1000$.

On an identical grid, Ghia et al. obtained a Strouhal number for the 15-deg case of 0.18 with a minimum lift coefficient of about 0.67 and a maximum of about 1.05 (Ref. 20). For the 30-deg case, the Strouhal number of 0.166 from the present method is very similar to the average Strouhal number of about 0.17 obtained by Ghia et al. In addition, the behavior of the cycles is similar, exhibiting two different minimum and maximum lifts in a cyclic fashion, indicating a subharmonic frequency of oscillation. The extremum values of lift are different, however. The peak lift coefficients from Ghia et al. are, in order: 1.9, 0.98, 1.57, and 0.80. Present thin-layer results give 1.22, 0.96, 1.17, and 0.92.

Unsteady Turbulent Airfoil Flow

Rumsey[10] previously used the central-difference code of Pulliam to analyze the flow about a NACA 0012 airfoil at 18 and 19.4 deg and found the flows to be unsteady and periodic with a Strouhal number of about 0.03. Present upwind difference results at 18 deg yield an unsteady flow with the same Strouhal number of 0.03. However, present results at 25 deg on a 201×65 grid with a time step of 0.001 indicate a nearly steady solution, with only a small nonperiodic variation in lift

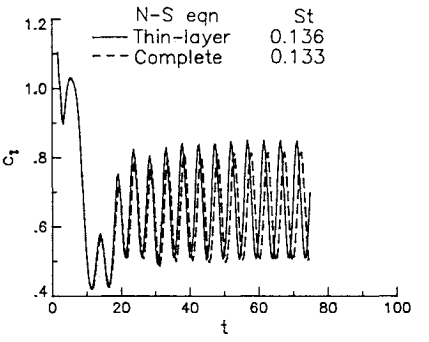

Fig. 11 Lift-coefficient time history for 12% Joukowski airfoil; $\alpha = 15$ deg; $M = 0.4$; $Re = 1000$.

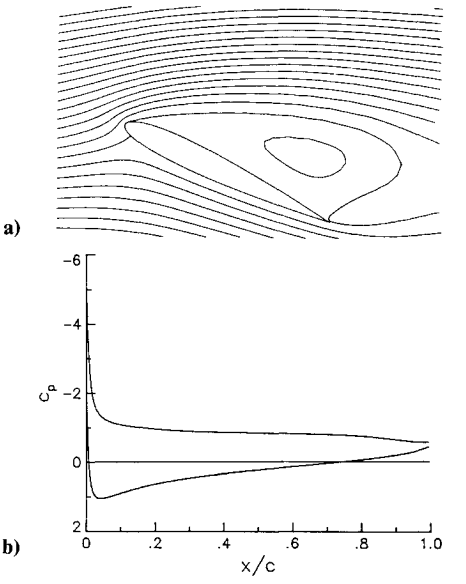

Fig. 12 Turbulent computation for NACA 0012 airfoil; $\alpha = 25$ deg; $M = 0.3$; $Re = 1 * 10^6$. a) stream-function contours; b) pressure distribution.

about an average value of about 1.07. Experimental results of Loftin[21] for a NACA 0012 airfoil at $M = 0.5$ and $Re = 1.3 * 10^6$ show a lift coefficient of about 1.0 at this angle of attack. It is possible that at this angle of attack the airfoil is past the region, just beyond maximum lift, where significant oscillatory behavior is present (see Jones[6] and Rumsey[10]). Results are given in Figs. 12a and b. A massively separated region is evident above the airfoil. The peak pressure coefficient has a value of about -4.7.

Concluding Remarks

An implicit finite-volume upwind Navier-Stokes code has been used for several steady and unsteady computations. Both the thin-layer and complete formulations of the Navier-Stokes equations have been used, and an evaluation has been made of the differences between their results. A systematic grid and time refinement study was conducted for laminar circular cylinder flow at a Reynolds number of 174, including the effect of grid density, grid extent, and time step on the Strouhal number. The thin-layer and complete Navier-Stokes formulations give Strouhal numbers of 0.189 and 0.195, respectively, in excellent agreement with the experimental range of 0.174-0.196. Thin-layer equations produce a larger variation in the oscillatory lift coefficient, -0.8-0.8, as opposed to -0.6-0.6 for complete equations. The present method yields accurate wake shapes in comparison to experiment for early times on an impulsively started laminar flow over a cylinder.

Computations for the inclined plate tested experimentally by Fage and Johansen predict Strouhal numbers comparable to experimentally measured values at 20- and 30-deg angle of attack. The average pressure coefficient over the plate at 30 deg shows good agreement with experiment.

Unsteady laminar flow computations over a NACA 0012 airfoil at 20-deg angle of attack have been made over a range of Reynolds numbers. The Strouhal number shows little change with Reynolds number, although the periodic lift levels change appreciably. Unsteady calculations for a Joukowski airfoil indicate differences between the thin-layer and complete Navier-Stokes results similar in nature to those observed for the circular cylinder: Strouhal numbers are nearly identical, but the thin-layer equation predicts a greater minimum-maximum lift variation. All Strouhal numbers obtained for airfoils are somewhat higher than the general airfoil Strouhal number of 0.150 defined experimentally by Tyler. Turbulent flow computations of a NACA 0012 airfoil at 25 deg predict a nonperiodic, massively separated solution, in good agreement with the experiments of Loftin.

References

[1]Thom, A., "The Flow Past Circular Cylinders at Low Speeds," *Proceedings of the Royal Society of London Series A*, Vol. 141, 1933, pp. 651–669.

[2]Morkovin, M., "Flow Around Circular Cylinder—A Kaleidoscope of Challenging Fluid Phenomena," *ASME Symposium on Fully Separated Flows*, 1964, pp. 102–118.

[3]Roshko, A., "On the Development of Turbulent Wakes from Vortex Streets," NACA TN-2913, 1953.

[4]Fage, A. and Johansen, F., "On the Flow of Air Behind an Inclined Flat Plate of Infinite Span," *Proceedings of the Royal Society, Series A*, Vol. 116, 1927, pp. 170–197.

[5]Tyler, E., "Vortex Formation Behind Obstacles of Various Sections," *Philosophical Magazine S.7.*, Vol. 11, No. 72, 1931, pp. 849–890.

[6]Jones, M., "Stalling," *Journal of the Royal Aeronautical Society*, Vol. 38, No. 285, 1934, pp. 763–770.

[7]Ghia, K., Osswald, G., and Ghia, U., "Analysis of Two-Dimensional Incompressible Flow Past Airfoils Using Unsteady Navier-Stokes Equations," *Third Symposium on Numerical and Physical Aspects of Aerodynamic Flows*, California State Univ., 1985, pp. 6.29–6.43.

[8]Osswald, G., Ghia, K., and Ghia, U., "An Implicit Time-Marching Method for Studying Unsteady Flow with Massive Separation," AIAA Paper 85-1489, 1985.

[9]Lecointe, Y. and Piquet, J., "Unsteady Viscous Flow Round Moving Circular Cylinders and Airfoils," AIAA Paper 85-1490, 1985.

[10]Rumsey, C., "Time-Dependent Navier-Stokes Computations of Separated Flows Over Airfoils," AIAA Paper 85-1684, 1985.

[11]Pulliam, T., Jespersen, D., and Childs, R., "An Enhanced Version of an Implicit Code for the Euler Equations," AIAA Paper 83-0344, 1983.

[12]Van Leer, B., "Flux-Vector Splitting for the Euler Equations," ICASE Rept. 82-30, 1982; see also *Lecture Notes in Physics*, Vol. 170, 1982, pp. 507–512.

[13]Baldwin, B. and Lomax, H., "Thin Layer Approximation and Algebraic Model for Separated Turbulent Flows," AIAA Paper 78-257, 1978.

[14]Thomas, J. and Salas, M., "Far-Field Boundary Conditions for Transonic Lifting Solutions to the Euler Equations," AIAA Paper 85-0020, 1985.

[15]Anderson, W., Thomas, J., and Van Leer, B., "A Comparison of Finite Volume Flux Vector Splittings for the Euler Equations," AIAA Paper 85-0122, 1985.

[16]Cook, P., McDonald, M., and Firmin, M., "Airfoil RAE 2822—Pressure Distributions, and Boundary Layer Wake Measurements," AGARD Advisory Rept. 138, Paper A6, 1979, pp. A6.1–A6.77.

[17]Swanson, R. Jr., Turkel, E., and Vatsa, V., "A Multistage Time-Stepping Scheme for the Thin-Layer Navier-Stokes Equations," *Langley Symposium on Aerodynamics*, Vol. 1, NASA CP-2397, 1985, pp. 109–136.

[18]Blottner, F., "Variable Grid Scheme Applied to Turbulent Boundary Layers," *Computer Methods in Applied Mechanics and Engineering*, 1974, pp. 179–194.

[19]Bouard, R. and Coutanceau, M., "The Early Stage of Development of the Wake Behind an Impulsively Started Cylinder for $40 < Re < 10^4$," *Journal of Fluid Mechanics*, Vol. 101, Pt. 3, 1980, pp. 583–615.

[20]Osswald, G., private communication, 1985.

[21]Loftin, L. Jr., "Airfoil Section Characteristics at High Angles of Attack," NACA TN-3241, 1954.